Turkish Journal of Electrical Engineering & Computer Sciences

http://journals.tubitak.gov.tr/elektrik/

Research Article

Turk J Elec Eng & Comp Sci
(2019) 27: 1885 – 1895

doi:10.3906/elk-1805-77

Hydrogen production system with fuzzy logic-controlled converter

Salih NACAR[1,*], **Selim ÖNCÜ**[2]

[1]Electrical Program, Taşköprü Vocational High School, Kastamonu University, Kastamonu, Turkey

[2]Department of Electrical and Electronics Engineering, Faculty of Engineering, Karabük University, Karabük, Turkey

Received: 13.05.2018 • **Accepted/Published Online:** 06.01.2019 • **Final Version:** 15.05.2019

Abstract: Electrolyte current must be controlled in the water electrolysis systems. For this purpose, the power converter for the cell stack of the electrolyzer used in industrial hydrogen production is realized. A series resonant converter, which is suitable for high input voltage and low output current applications, is used as power stage of the electrolyzer. The high-frequency transformer is used for the impedance matching. While the system is running, the electrical resistance of the electrolyzer changes continuously; thus, fuzzy logic controller (FLC) is used to control the output current of the power converter. In this study, a 700-W converter prototype is designed and controlled by the frequency modulation technique in the range of 290–360 kHz. The converter is tested for different output currents and it is observed that the power switches are turned on under soft switching conditions while FLC closely follows reference inputs.

Key words: Fuzzy logic controller, resonant converter, soft switching, electrolysis

1. Introduction

Hydrogen can be produced easily in high purity by electrolysis of water. The basic function of electrolysis is to separate the water components, which are oxygen and hydrogen. The hydrogen produced by this method is proportional to applied direct current to electrolyte, which is a chemical compound and can conduct the electric current [1, 2]. Especially, it increases interest in the DC–DC converters that are used to perform controlled power flow in the systems. The systems are constituted to produce hydrogen by electrolysis [2–13]. The converters can be controlled by pulse width modulation (PWM) [2–7] or resonant switching techniques [8–13]. The studies on DC–DC converters usually aim at improving efficiency and reducing cost and volume [14–22]. Higher power density can be achieved by increasing the switching frequency of the converter. However, increasing the switching frequency (f_s) in the PWM control technique leads to increase in the switching losses, electromagnetic interference, and stresses on the switches [17, 18]. In resonant converters, power switches can be soft-controlled instead of hard switching, which is in consequence of PWM switching. Soft switching is achieved by converting the square wave voltage across the switch or the square wave current flowing through the switch into the sinusoidal form obtained by using the LC resonance elements. [21, 22].

The load resonant converters can be classified into two main groups as series resonant converter (SRC) and parallel resonant converter (PRC) as regards to transfer of power from the resonance circuit [23]. The SRC is especially preferred for high input voltage and low output current applications [24, 25]. The resonance current is proportional to the load current. Along with reduction in the load, the resonance current also decreases, which leads to reduction in conducting and the switching losses. Also, since the series resonance capacitor blocks the

*Correspondence: snacar@kastamonu.edu.tr

DC components, the saturation of high-frequency transformer can be avoided [24, 26]. For the electrolysis applications, both isolated and nonisolated different converter topologies were used in previous studies [2–13].

The amount of hydrogen produced by the electrolysis method is directly proportional to the applied direct current to the electrolyte. Moreover, the electrical resistance of the electrolyzer varies considerably depending on the temperature and the concentration ratio [1]. Therefore, the output current of the converter should be controlled. The nonlinear systems can be controlled by FLC. In addition, in performing the output regulation, FLC is more robust than proportional integral differential (PID) controller against changing system parameters such as the reference value, the input voltage, and the load [27–31]. In this study, SRC is preferred for the power stage of the system since the output current is low-level. Also, FLC is selected as the control technique of SRC to regulate the current. The rule base of FLC, which has two inputs and one output, consists of 25 rules. It is operated by using a digital signal controller (DSC). The converter is designed to operate above the resonant frequency to increase the effectiveness of the resonance circuit functioning as a filter. Thus, the harmonics of the square wave voltage are effectively removed. Moreover, it is guaranteed that MOSFETs and rectifier diodes are turned on under soft switching conditions. The analysis of SRC is performed with the fundamental harmonic approximation (FHA) especially giving accurate results at the resonant frequency and above.

2. Electrolysis system with series resonant converter

The circuit structure of fuzzy logic controlled electrolysis system is shown in Figure 1. The system consists of a full bridge series resonant converter, high-frequency transformer (T), the rectifier circuit, a stack as DC load and a control circuit. The full bridge inverter stage produces a square wave voltage v_{ab} by driving of $M_{1\text{-}4}$ and $M_{2\text{-}3}$ switches alternately. The resonant circuit consists of the leakage inductance (L) of the high-frequency transformer and externally added resonant capacitor (C). The output of SRC is rectified and filtered with C_o capacitor, to obtain DC electrolysis current I_o.

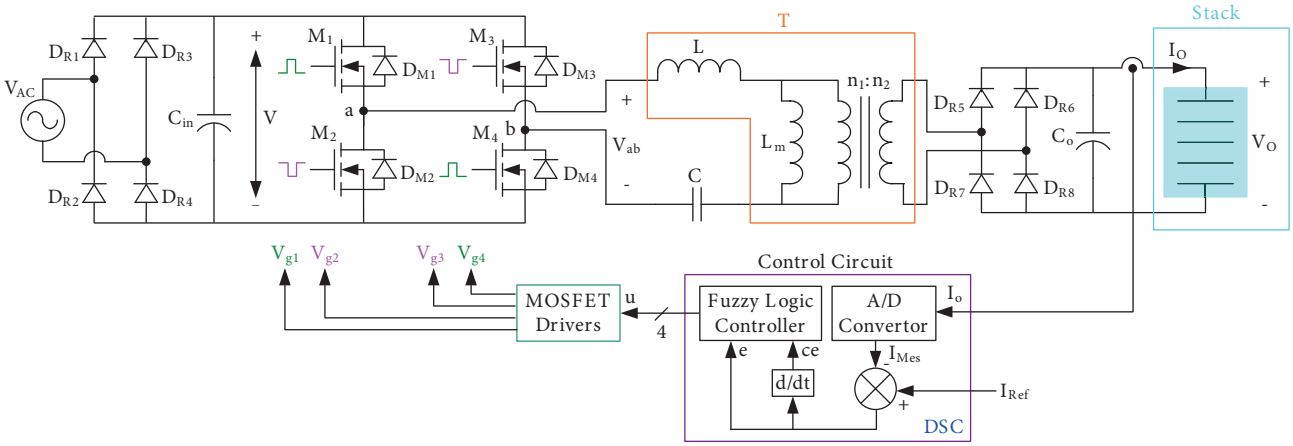

Figure 1. Fuzzy logic controlled electrolysis system.

2.1. SRC analysis

The fundamental harmonic approach (FHA) is used to determine the gain of the converter and the following assumptions are accepted in the analysis [32].

1. The circuit is operating under steady-state conditions.
2. The input/output filter capacitor is large enough for the constant voltage supply.
3. All circuit elements are ideal.
4. The secondary circuit is reflected as R_e to the primary side.

The equivalent circuit obtained from these assumptions is given in Figure 2. The voltage (v_e) across R_e is the reflected voltage to the primary side and obtained by multiplying the output voltage V_o by the conversion ratio "a" (n1/n2) of the transformer.

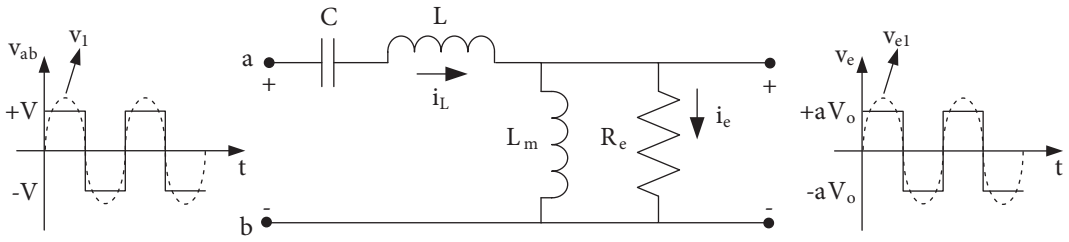

Figure 2. The equivalent circuit of SRC.

Since the magnetism inductance $L_m \gg L$, the effect of L_m at the resonance frequency (f_r) can be neglected and the equivalent circuit can be simplified as shown in Figure 3.

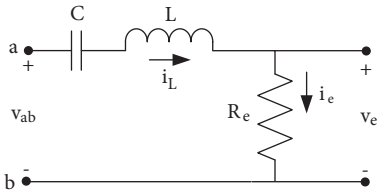

Figure 3. The simplified equivalent circuit of SRC.

As seen from the simplified equivalent circuit, the resonant circuit of the converter is a basic series RLC circuit. The resonant frequency and normalized frequency (f_n) by using the swtiching frequency (f_s) of the converter are

$$f_r = \frac{1}{2\pi\sqrt{LC}}, \tag{1}$$

$$f_n = \frac{f_s}{f_r}. \tag{2}$$

The quality factor of the converter is given in the following equation.

$$Q = \frac{2\pi f_r L}{R_e} \tag{3}$$

The value of equivalent resistance R_e is given in Eq. (4) [32].

$$R_e = \frac{V_{e1}}{I_e} = \frac{\frac{4aV_o}{\pi}}{\frac{I_o\pi}{2a}} = \frac{8a^2V_o}{\pi^2 I_o} \tag{4}$$

The gain of the simplified equivalent circuit is obtained by dividing the fundamental components of output and input voltages as follows [32].

$$M = \frac{V_{e1}}{V_1} = \frac{\frac{4aV_o}{\pi}}{\frac{4V}{\pi}} = \frac{V_o a}{V} = \frac{1}{\sqrt{1 + (\frac{X_L - X_C]}{R_e})^2}} \tag{5}$$

As given in Eq. (5), the gain is unity at f_r since the X_L and X_C reactances are equal. In this case, the series resonance current is pure sine. The frequency-gain curves for different quality factors are given in Figure 4. As seen from the curves, the converter has two different operation regions (ZCS and ZVS). Furthermore, the gain at f_r is independent of the load, and this is an important design criteria.

In the ZVS region, the gain is less than unity and the slope is negative, the MOSFETs turn on with zero voltage. This reduces turn-on switching losses. In ZCS region, switches turn off with zero current; however, turn-on losses increase and efficiency of the converter decreases.

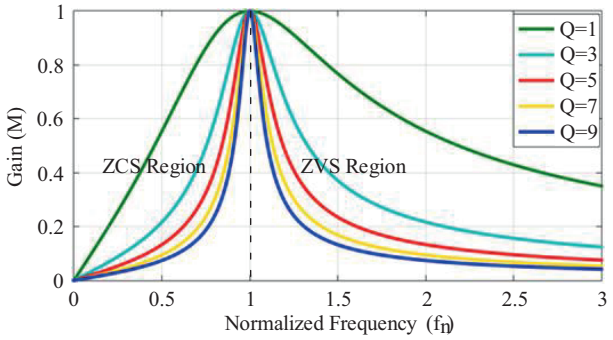

Figure 4. Normalized frequency-gain response for different Q values of SRC.

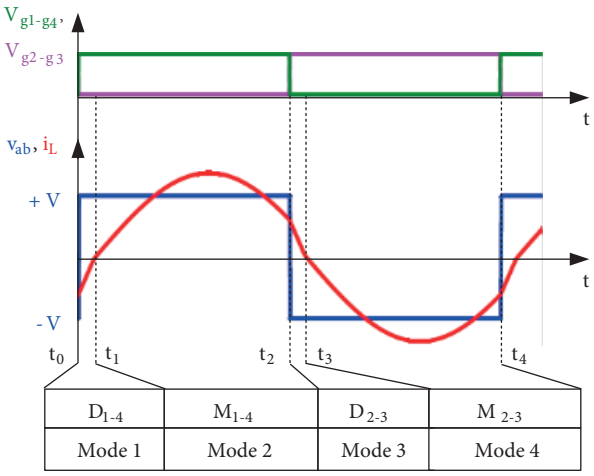

Figure 5. The operating intervals for $f_s > f_r$.

The operating intervals of the converter in ZVS region are given in Figure 5. The operating modes for ZVS region can be divided to four modes; Mode I ($t_0 \leq t < t_1$): When $M_{2\text{-}3}$ are turned off at t_0, the body diodes $D_{1\text{-}4}$ conduct the negative i_L. In this case, the voltages at the terminals of $M_{1\text{-}4}$ are clamped to the diode voltage so that the ZVS condition for these MOSFETs is formed. Mode II ($t_1 \leq t < t_2$): As soon as $D_{1\text{-}4}$ are turned off at t_1, $M_{1\text{-}4}$ are turned on under ZVS condition. In this mode, the resonant current is positive. Mode III ($t_2 \leq t < t_3$): This mode is similar to Mode I. When $M_{1\text{-}4}$ are turned off at t_2, the $D_{2\text{-}3}$ diodes are conducted by the positive i_L. Mode IV ($t_3 \leq t < t_4$): This mode is similar to Mode II. When $D_{2\text{-}3}$ are turned off at t_3, $M_{2\text{-}3}$ are turned on with ZVS. Thus, the operation of converter completes in 4 different modes. After t_4, the operation modes of the converter repeat from Mode 1 to Mode 4.

2.2. The fuzzy logic control system

The control of systems is usually difficult for continuously changing input/output parameters. Therefore, the control of systems, which are mathematically difficult to analyze and have variable parameters, can be realized

with fuzzy logic controller. Because the expert knowledge and FLC units (fuzzification, rule base, inference engine, and defuzzification), which are operated according to certain rules, are sufficient to control a system.

The output parameter for the proposed FLC electrolysis system is electrolysis current (I_o) and the control variable is the switching period (T_s). The dynamic behavior of the system required to form the rule base is given in Figure 6.

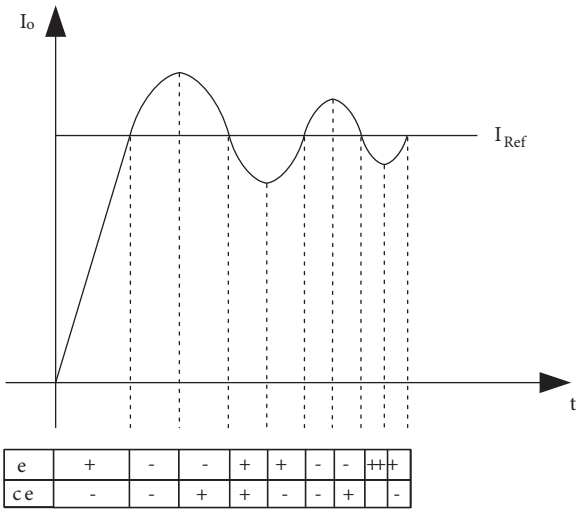

Figure 6. The dynamic behavior of the system.

The control circuit locks the electrolysis current to the reference value with fuzzy logic controller. The inputs of FLC; error (e) is the difference between the reference value and the measured value, the error in the change (ce) is the difference between the current error and the previous error. The change in the switching period (u), which is the control variable, is determined by e and ce. The control signals are produced by the DSC's high-speed PWM module.

The input and output linguistic variables N, Z, P, B, and S of FLC are negative, zero, positive, big, and small, respectively. The rule base of FLC is formed by the IF-THEN rules. For example, if e is NB and ce is PS then u is NB. The rule base, which is established by considering the dynamic behavior of the system with the IF-THEN rules, is given in Table 1.

Table 1. Rule base.

e/ce	**NB**	**NS**	**Z**	**PS**	**PB**
NB	NB	NB	NB	NB	Z
NS	NB	NS	NS	Z	PB
Z	NB	NS	Z	PS	PB
PS	NB	Z	PS	PS	PB
PB	Z	PB	PB	PB	PB

As seen in Figure 7, triangular and trapezoid membership functions are used in the input and output variables of FLC. While the x-axis shows the membership values of variables, the y-axis shows the membership level of the corresponding variable. In FLC, min-max (Mamdani) is used as the fuzzy inference method and the center of gravity method is used as the defuzzification method.

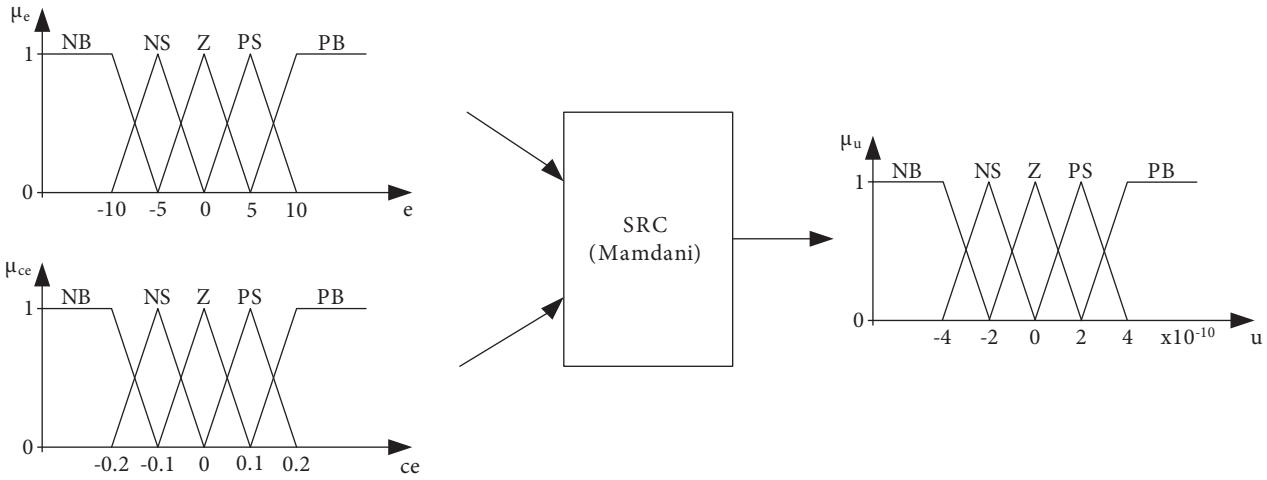

Figure 7. Input and output membership functions of FLC.

Analog integrated circuits, PLC and DSP are used for the control of converters in studies carried out for electrolysis [5–7, 11, 12, 26]. Among the microcontroller systems such as PLC and DSP, the low-cost DSPIC is preferred to control the electrolysis system.

3. Experimental study

The experimental setup for electrolysis is given in Figure 8.

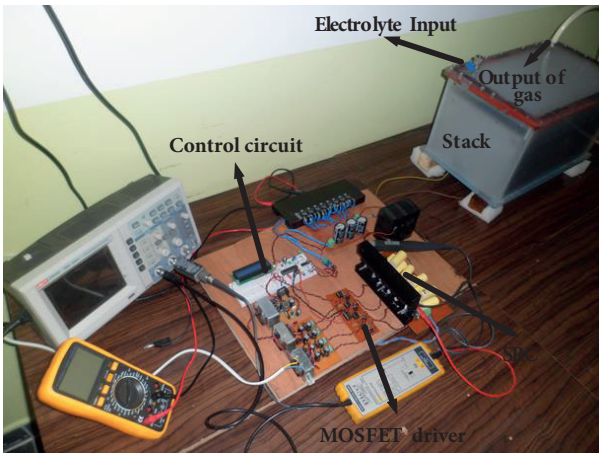

Figure 8. The experimental setup.

To set the hydrogen production system, the alkaline electrolysis stack consisting of 15 serial cells is filled with 18 L of electrolyte prepared. The electrolyte is composed of water and 30% potassium hydroxide, which is used to increase the conductivity of water. Prior to performing the closed-loop control of the system, voltages of 0 to 35 V are applied to the stack and the current is measured to obtain the load characterization of the stack. The stack and current-voltage curve from the experimental measurements are given in Figure 9.

The input voltage (V) of the converter is obtained by rectified mains. Under nominal conditions, the electrolysis current value is set to 20 A. When considering the losses, it is accepted that the converter works

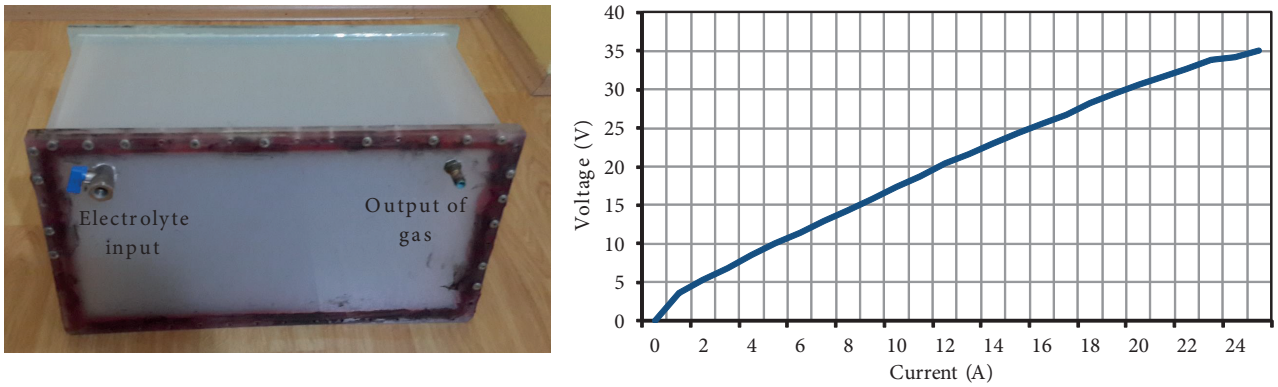

(a) (b)

Figure 9. The alkaline electrolyzer, a) Physical box of electrolyzer appearance and b) The current-voltage curve.

with 95% efficiency for the full load at f_r. However, at nominal conditions, the converter gain M is accepted to be 0.9 in order to guarantee ZVS. The parameters of the converter are given in Table 2.

Table 2. Rule base.

V	310 V	L_m	800 μH
V_o	33-36 V	C	10 nF
P_o	700 W	f_r	218 kHz
a	8:1	M_{1-4}	IRFP460
L	53 μH	D_{R5-8}	DSEI60-06A

In the hydrogen production system, a low-cost 16-bit DSPIC33FJ16GS502 digital signal controller is used to operate the control algorithm, generate the gate signals and digitize the feedback information. DSC is more functional and flexible than analog integrated circuits and it is cheaper, easier to access and use than PLC and DSP. The electrolysis current is measured by the hall-effect sensor and then digitized by the ADC module of DSC.

In order to observe whether the current applied to the stack for hydrogen production at different rates could follow the reference value, the system is initially operated for the reference current value of 15 A, then the system is stopped and operated again after the reference current value is changed to 20 A. The stack current and voltage for these reference values are given in Figure 10.

The current of stack closely follows the changed reference current value by the FLC. Figure 11 shows the resonant current and voltage according to the changed reference value. It is seen that amplitude of the current changes with the changing reference current. This is accomplished by controlling the switching frequency from 360 to 290 kHz. Thus, the power control of the converter from 400 to 700 W is carried out by changing the switching frequency.

The drain current (i_{M1}) and drain-source voltage (v_{M1}) waveforms of the MOSFET in the full bridge circuit are given in Figure 12.

According to Figure 12, the MOSFET is switched on with zero voltage. To show the validity and robustness of proposed FLC controller, the reference value is changed while the electrolysis process is continuing, as shown in Figure 13.

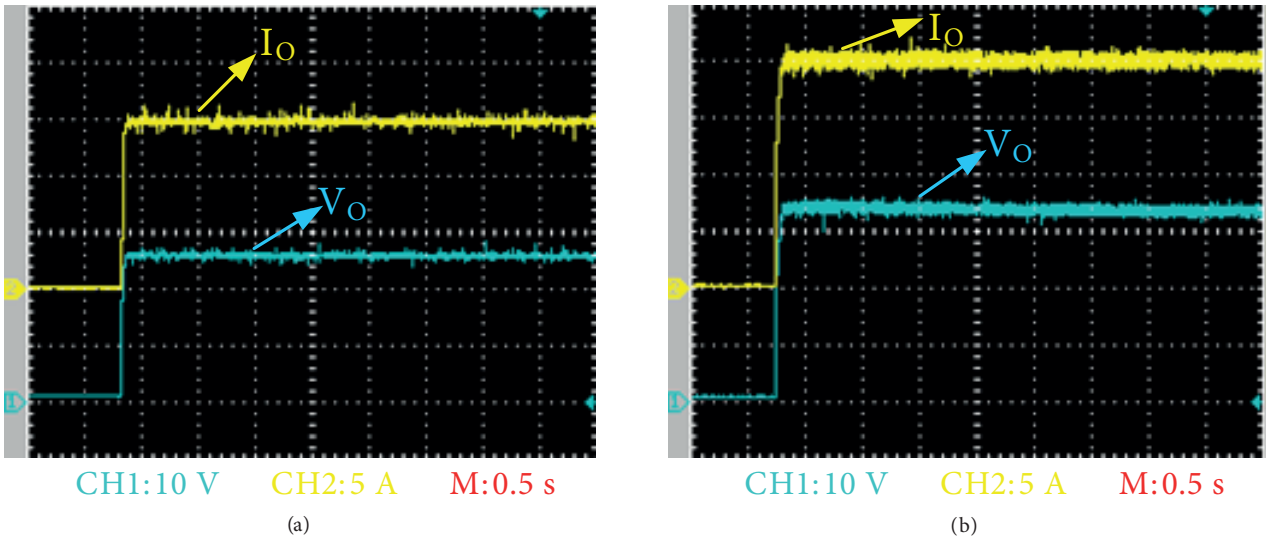

Figure 10. The current and voltage of the stack for different references values, a) for 15 A and b) for 20 A.

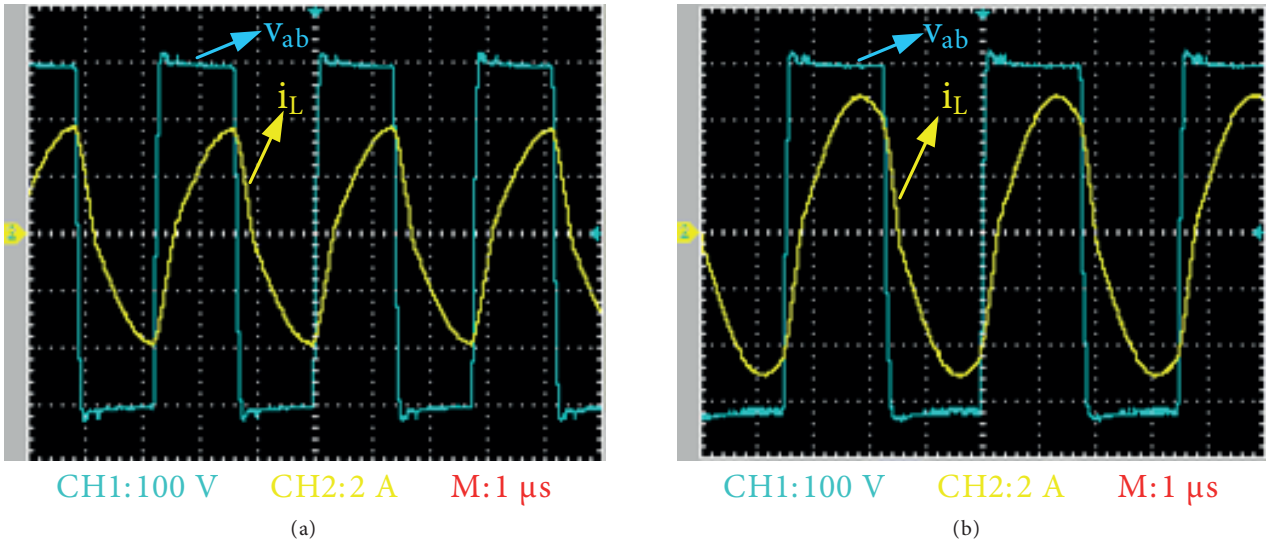

Figure 11. The resonant current and inverter voltage for different references values, a) for 15 A and b) for 20 A.

At the start, the reference value is selected as 15 A and then changed to 20 A, and the reference value is changed to the initial value 15 A again. According to Figure 13, the FLC continues to follow the reference value even if the reference value is changed while the system continues to operate.

4. Conclusions

In this study, the FLC-controlled SRC is designed to produce hydrogen at the desired rates from the electrolysis stack. The FLC regulates the output current with frequency modulation at around 300 kHz switching frequency. Low switching losses, low electromagnetic interference, and high power density are the advantages of the designed SRC. FLC algorithm closely follows the reference value under nonlinear variable conditions. DSC can easily achieve FLC method for high-frequency resonant converter. The output power of the converter is controlled between 700 and 400 W for the switching frequency range between 290 and 360 kHz despite changing load

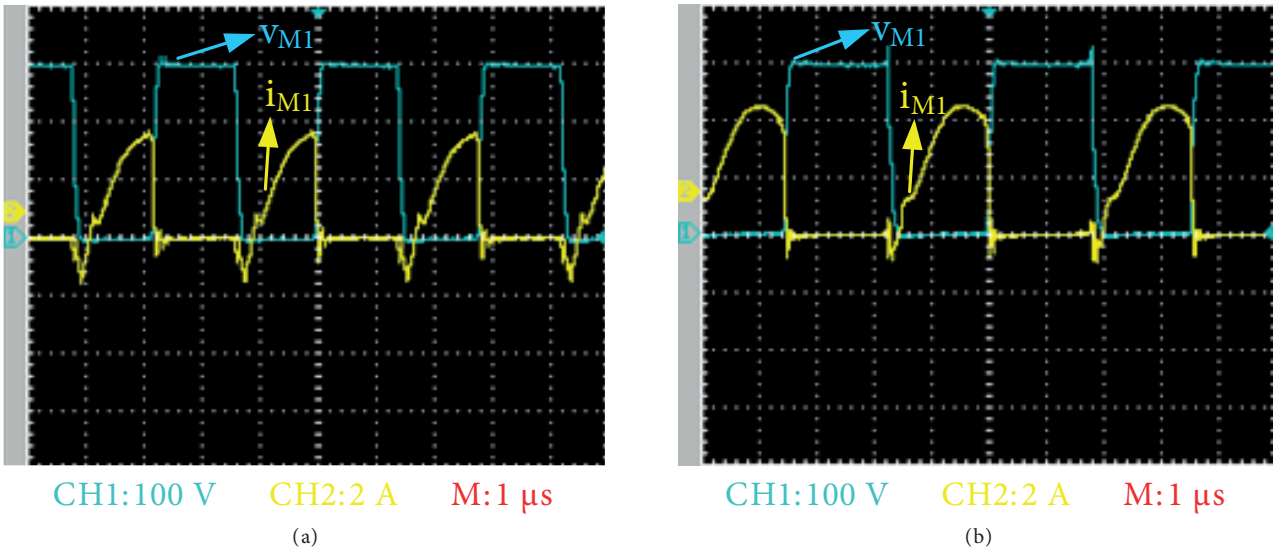

Figure 12. The current and voltage of the switch for different reference values, a) for 15 A and b) for 20 A.

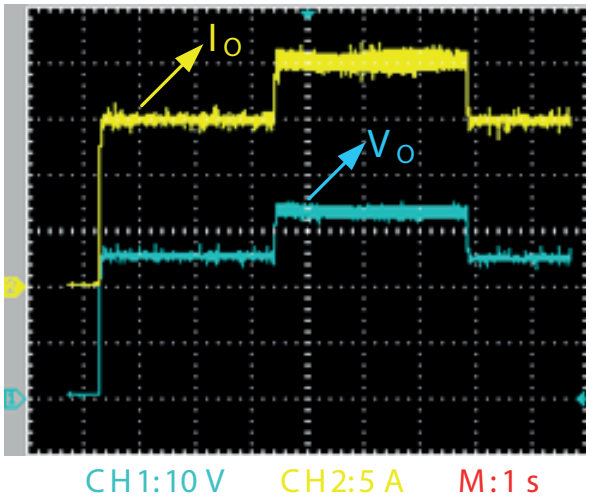

Figure 13. The robustness of FLC for changing reference values.

and reference current values. Finally, the digital control of the designed system is carried out by means of the low-cost microcontroller.

Acknowledgment

This research was supported by Karabük University Research Fund (KBUBAP-17-DR-264).

References

[1] Ulleberg Ø. Modeling of advanced alkaline electrolyzers: a system simulation approach. Int J Hydrogen Energy 2003; 28 (1): 21-33.

[2] Dahbi S, Aboutni R, Aziz A, Benazzi N, Elhafyani M et al. Optimised hydrogen production by a photovoltaic-electrolysis system DC/DC converter and water flow controller. Int J Hydrogen Energy 2016; 41 (45): 1-9.

[3] Garrigos A, Lizan JL, Blanes JM, Gutierrez R. Combined maximum power point tracking and output current control for a photovoltaic-electrolyser DC/DC converter. Int J Hydrogen Energy 2014; 39 (36): 20907-20919.

[4] Koiwa K, Umemura A, Takahashi R, Tamura J. Stand-alone hydrogen production system composed of wind generators and electrolyzer. In: 2013-39th Annual Conference of the IEEE Industrial Electronics Society; Vienna, Austria; 2013. pp. 1873-1879.

[5] Vinnikov D, Hõimoja H, Andrijanovits A, Roasto I, Lehtla T et al. An improved interface converter for a medium-power wind-hydrogen system. In: 2009 International Conference on Clean Electrical Power; Capri, Italy; 2009. pp. 426-432.

[6] Garrigós A, Blanes JM, Carrasco JA, Lizán JL, Beneito R et al. 5 kW DC/DC converter for hydrogen generation from photovoltaic sources. Int J Hydrogen Energy 2010; 35 (12): 6123-6130.

[7] Ursua A, San Martin I, Sanchis P. Design of a programmable power supply to study the performance of an alkaline electrolyser under different operating conditions. In: 2012 IEEE International Energy Conference and Exhibition; Florence, Italy; 2012. pp. 259-264.

[8] Török L, Nielsen CK, Munk-Nielsen S, Rømer C, Flindt P. High efficiency electrolyser power supply for household hydrogen production and storage systems. In: 2015 17th European Conference on Power Electronics and Applications; Geneva, Switzerland; 2015. pp. 1-9.

[9] Babu RSR, Henry J. A comparative analysis of DC-DC converters for renewable energy system. In: Proceedings of The International Multi Conference of Engineers & Computer Scientists; Hong Kong, China; 2012. pp. 1020-1025.

[10] Gautam DS, Bhat AKS. A comparison of soft-switched DC-to-DC converters for electrolyzer application. IEEE T Power Electr 2013; 28 (1): 54-63.

[11] Chandrasekhar P, Reddy SR. Performance of soft-switched DC-DC resonant converter for Electrolyzer. In: 2011 4th International Symposium on Resilient Control Systems; Boise, ID, USA; 2011. pp. 95-100.

[12] Cavallaro C, Chimento F, Musumeci S, Sapuppo C, Santonocito C. Electrolyser in H2 self-producing systems connected to DC link with dedicated phase shift converter. In: 2007 International Conference on Clean Electrical Power; Capri, Italy; 2007. pp. 632-638.

[13] Cavallaro C, Cecconi V, Chimento F, Musumeci S, Santonocito C et al. A phase-shift full bridge converter for the energy management of electrolyzer systems. In: 2007 IEEE International Symposium on Industrial Electronics; Vigo, Spain; 2007. pp. 2649-2654.

[14] Hossain MZ, Rahim NA. Recent progress and development on power DC-DC converter topology, control, design and applications: A review. Renew Sust Energy Rev 2018; 81 (1): 205-230.

[15] Oncu S, Karafil A. Pulse density modulation controlled converter for PV systems. Int J Hydrogen Energy 2017; 42 (28): 17823-17830.

[16] Ting NS, Sahin Y, Aksoy I. Analysis, design and implementation of a zero-voltage-transition interleaved boost converter. J Power Electron 2017; 17 (1): 41-55.

[17] Hua G, Leu CS, Jiang Y, Lee FCY. Novel zero-voltage-transition PWM converters. IEEE T Power Electr 1994; 9 (2): 213-219.

[18] Bodur H, Bakan AF. A new zvt-pwm dc-dc converter. IEEE T Power Electr 2002; 17 (1): 40-47.

[19] Bal G, Öztürk N. A novel control technique for soft-switching sinusoidal pulse width modulation inverter. Electr Pow Compo Sys 2011; 39 (1): 35-45.

[20] Liu KH, Oruganti R, Lee FCY. Quasi-resonant converters-topologies and characteristics. IEEE T Power Electr 1987; 2 (1): 62-71.

[21] Lee FC. High-frequency quasi-resonant converter technologies. P IEEE 1988; 76 (4): 377-390.

[22] Liu KH, Lee FC. Zero-voltage switching technique in DC/DC converters. IEEE T Power Electr 1990; 5 (3): 293-304.

[23] Todd PC, Lutz RW. A practical parallel loaded resonant power supply. In: Applied Power Electronics Conference and Exposition; New Orleans, Louisiana, USA; 1986. pp. 90-97.

[24] Steigerwald RL. A comparison of half-bridge resonant converter topologies. IEEE T Power Electr 1988; 3 (2): 174-182.

[25] Rossetto L. A simple control technique for series resonant converters. IEEE T Power Electr 1996; 11 (4): 554-560.

[26] Deying G, Yingying L. Control of hydrogen production by water electrolyzer based on self-turning fuzzy-PI. In: 2012 24th Chinese Control and Decision Conference; Taiyuan, China; 2012. pp. 1719-1721.

[27] Sharma K, Palwalia DK. Robust controller design for DC-DC converters using fuzzy logic. In: 2017 4th International Conference on Signal Processing, Computing and Control; Solan, India; 2017. pp. 477-481.

[28] Kesler S, Doser TL. Analysis, a voltage regulation system for independent load operation of stand alone self-excited induction generators. J Power Electron 2016; 16 (5): 1869-1883.

[29] Buccella C, Cecati C, Latafat H, Razi K. Comparative transient response analysis of LLC resonant converter controlled by adaptive PID and fuzzy logic controllers. In: IECON 2012-38th Annual Conference on IEEE Industrial Electronics Society; Montreal, QC, Canada; 2012. pp. 4729-4734.

[30] Bal G, Bekiroğlu E, Demirbaş Ş, Colak I. Fuzzy logic based DSP controlled servo position control for ultrasonic motor. Energ Convers Manage 2004; 45 (20): 3139-3153.

[31] Madhanakkumar N, Sivakumaran TS, Sri DD. Performance analysis of PI and fuzzy control for resonant converter incorporating boost converter. In: 2014 International Conference on Science Engineering and Management Research; Chennai, India; 2014. pp. 1-8.

[32] Bhat AKS. Analysis and design of LCL-type series resonant converter. IEEE T Ind Electron 1994; 41 (1): 118-124.